Control Analysis of Building Under Construction from Indoor Mobile Mapping Systems

Patricia González-Cabaleiro[1], Rosa M. Túñez-Alcalde[1], Muataz S. A. Albadri[1], Antonio Fernández[1], Lucía Díaz-Vilariño[1]

[1] CINTECX, Universidade de Vigo, GeoTECH Group. 36310 Vigo, Spain
(patricia.gonzalez.cabaleiro, rosamaria.tunez, muatazsafaaabed.albadri, antfdez, lucia)@uvigo.gal

Keywords: 3D Modelling, Scan-to-BIM, Scan-vs-BIM, Indoor Mobile Mapping, Digital Twins, Construction Monitoring.

Abstract

During the execution phase of construction projects, quality defects arise due to various factors such as human intervention, technical aspects, logistical issues and environmental influences. Early detection of these defects is imperative to minimize their impact and prevent possible delays, increased costs and safety hazards. This paper explores the effectiveness of indoor mobile laser scanners for geometric quality control, adhering to established European technical norms and Spanish standards. Our developed approach presents a simple method for rapid assessment, capable of identifying vertical deviations in columns and walls, axis deviation in columns, flatness deviation in horizontal planes and level deviation using LIDAR data from Mobile Mapping Systems. This methodology has been validated through a real-world case study, demonstrating its practical applicability.

1. Introduction

There are different types of buildings depending on their intended use, such as offices, residential buildings, or industrial facilities (Li et al., 2022). Despite their differences, they all share the common requirement for periodic inspections and progress monitoring to ensure adherence to standards and jurisdictional requirements (Mirzaei et al., 2023b). However, inadvertent can arise due various factors at any time of the process. (Jingmond and Ågren, 2015) suggest that many defects in the construction industry stem more from internal organizational factors rather than technical causes. Although market factors and technical issues do have an impact, they are often consequences of deeper organizational problems. Nevertheless, (Love et al., 2022) propose an alternative perspective, emphasizing the significant impact of human factors within the context of human, technical, logistical, and environmental influences. They particularly highlight how deteriorated human cognition, such as fatigue, stress, or boredom, affects our capabilities and leads to errors, potentially compromising the quality of the final result. Therefore, it is imperative to quickly identify errors to prevent them from causing major disasters (Matthews et al., 2021).

These errors are classified based on their geometrical and spatial aspects (Delval et al., 2023) and include surface-based defects, easily identified through visual inspection, and volume-based defects, which encompass dimensional discrepancies, such as flatness or section issues, as well as positional deviations, which involve XYZ position and orientation regularities like vertical deviation. Given our focus on geometric defects, Geometric Quality Control assumes a crucial role in the early identification of these issues during construction. Its impact lies not only in preventing costly rework, extensive repairs, and potential budget increase (Love et al., 2022) but also in ensuring the safety, durability, and functionality of structures (Bueno and Bosché, 2023). However, conventional quality control methods in construction present significant challenges (Mirzaei et al., 2023a). They are typically manual, inefficient, and require highly specialized personnel, resulting in time-consuming processes and increased costs. Moreover, current manual building compliance inspections frequently suffer from insufficient coverage, high costs, and reliance on subjective measurements. These limitations contribute to their ineffectiveness in identifying defects early in the construction process, leading to undetected issues persisting until later stages of construction or even into the maintenance phase (Akinci et al., 2006). Thus, there is a growing demand for more efficient and accurate methods to inspect structural works and monitor damage progression (Mirzaei et al., 2023b). This had led to the extensive adoption of building information models (BIMs) generated from laser scanner point cloud data to ensure both, completeness, and accuracy in the quality control of the model (Anil et al., 2013).

The past few decades have witnessed a dramatic drop in the price of scanning technologies, while simultaneously evolving into different types of devices, moving from the costly tripod-mounted scanners to backpack systems, handheld devices, and currently, smartphone integrations. High-speed scanning technology evolution produces new possibilities for quick and automatic inspections of defects in buildings under construction. On one hand, Indoor Mobil Mapping Sensors are characterized by their high efficiency in terms of speed and data completeness, but still they are poor in complying with technical requirements related to quality control of buildings under construction. Hence, the success of automated construction quality inspections relies on finding a compromise between speed and accuracy of data acquisition and data accuracy.

The present research focuses on exploring the capabilities of indoor mobile laser scanners for geometrical quality control based on the technical requirements established in existing norms. It introduces a method for the rapid analysis of level deviation, vertical deviation for walls and columns, flatness deviation in horizontal planes and axis deviation between columns. Then the methodology is validated through a real-world case study, which consists in a building under construction, demonstrating its practical application and effectiveness in identifying deviations and evaluating compliance with standards.

This paper is organized as follows. Section 2 provides a review of different methods to automatically detecting geometric defects in buildings employing scanning technologies. Section 3 outlines the developed approach, which includes four deviation analysis: level, flatness, vertical and axis deviation. Section 4 reveals the results obtained from applying the method in a real-world case study. Finally, Section 5 offers concluding remarks.

2. Related work

In recent years, numerous papers have focused on automatically detecting geometric defects in buildings under construction using laser scanning, with most utilizing both terrestrial laser scanners (TLS) and total stations. These studies have explored methods for identifying surface deviations, classified as dimensional defects, and vertical and axis deviations, classified as positional defects, all of them within the geometrical deviations category. Among these approaches, various methods have been developed to detect surface deviations. Damage Detection (Mohammadi, 2019), for instance, is a method that computes three surface descriptors (surface, normal, and curvature variation), each contributing to a probability distribution function for deviation identification. Then, an algorithm evaluates the potential damage by cross-referencing anomalies identified by all descriptors.

In contrast, (Suchocki et al., 2008) present two distinct methodologies: the Spatial Intersection and 3D polar. The Spatial Intersection method targets characteristic points on the surface, typically at the corners of the windows or other prominent features, forming a grid pattern for systematic observation. Conversely, the 3D Polar method involves measuring form a single position multiple point cloud. Unlike the Spatial Intersection, which relies on simultaneous measurements from multiple points, the 3D Polar method requires manually pointing the instrument to each observed point sequentially. This approach creates a detailed three-dimensional model for visualizing all the deviations.

Other authors have devised approaches such as Flatness Quality Assessment (Fu et al., 2022) for evaluating, specifically, concrete surfaces. This method entails capturing point cloud data, fitting planes to establish a reference for deviation calculation and calculating deviations, which are subsequently visualized using color-coded maps. Similarly, for component surfaces, deviations are calculated based on reference points from as-designed models, which are aligned with scanned data using algorithms like 4PCS and IPC. Additionally, (Kim and Chang, 2014) propose the concrete spalling defect-detection method, which utilizes defect-sensitive features to identify quality issues. The method subdivides the surface, computes defect indices and establishes a diagnosis threshold based on intact subdivisions. Initial defect localization is followed by recursive refinement and defect quantification for estimating total volume loss.

Recent advancements have incorporated deep learning techniques to enhance efficiency as seen in the Flatness Quality and Vertical Assessment (FQVA) method (Li et al., 2022). This approach to flatness assessment combines elements from both, a method closer to the manual measurement denoted as virtual ruler-based method, and the reference plane-based method. By calculating the distance between each point and a given reference plane, it allows for the identification of defects. Additionally, the FQVA method aids in evaluating alignment and ensuring compliance with standards by calculating the angle between normal vectors and floor surfaces in the provided point cloud data.

Aside from techniques aimed at detecting surface deviations, many researchers have introduced approaches for identifying discrepancies between the as-planned and the as-built building such as the Point-to-point comparison method (Chen and Cho, 2018), Deviation Analysis method (Anil et al., 2013), (Moyano et al., 2022) method and Change Detection method (Girardeau-Montaut et al., 2005; Park et al., 2021). The first two methods can identify geometric, orientation and localization errors by generating deviation colour-coded maps from point cloud data that highlight these errors according to the degree of deviation. (Moyano et al., 2022), employ Dynamo for deviation analysis and validation of effectiveness for vertical assessment. Finally, the change detection, examined by (Girardeadu-Montaut et al., 2005) uses Hausdorff distance for a precise comparison between points. This metric measures the maximum distance between two sets of points, indicating their spatial separation, and is streamlined for efficiency using a light octree structure. This approach was further enhanced by (Park et al., 2021), which introduced an approach based on Modifiable Nested Octree (MNO) that subdivides 3D space into cubic cells enabling comparisons between similar elements in point cloud analysis providing a binary answer if the element is compliant on non-compliant with the standards.

Furthermore, ASDMCon (Advances Sensor-based Defect Management on Construction sites) is a model-based approach that employs feature-ontology and an attribute-ontology for identifying deviations, mapped to specific attributes or features (Akinci et al., 2006). Moreover, End-to-End method (Mirzaei et al., 2023a) automates extracting and assessing building structural members from point clouds. It utilizes distribution patterns and cross-section shapes of beams, columns and bracings for accurate detection. Through semantic segmentation and alignment, the method improves segmentation accuracy and obtains dimensions of the detected structural members.

Building on advancements in point cloud analysis, (Dąbrowski and Hubert Zienkiewicz, 2022) highlight the significance of considering factors such as height, inclination angle and symmetry axis offset to ensure precise outcomes when employing the Point Cloud Spatial Expansion (PCSE) method. This method rectifies inclination and extends the point cloud for comprehensive analysis, enabling detailed evaluation of geometric properties and symmetry parameters. Subsequent studies by (Dabrowski, 2022) focused on utilizing the PCSE method to introduce verticalization of point clouds, addressing distortions caused by inclined axes of sloped symmetrical objects. Utilizing Errors-In-Variables estimation ensured accurate determination of the symmetry axis. Extending this work, (Dabrowski et al., 2023) enhanced the method for evaluating the asymmetry and regularity of complex objects by estimating the symmetry axis through the identification of wall planes using *RANSAC* algorithm and their cross-section centroids.

Finally, recent research advancements in computer vision, machine learning and structural engineering, as highlighted by (Spencer et al., 2019), are transforming inspection and monitoring applications. The effectiveness of vision algorithms, including deep learning and optical flow, along with technologies like remote cameras and UAVs, aims to automate data pre-processing for improved infrastructure assessment efficiency. Ongoing research in condition-aware models, synthetic data generation and video estimation promises time-efficient, cost-effective and automated civil infrastructure monitoring, enhancing city safety and resilience.

3. Method

3.1 Preprocessing

Depending on the input point cloud, a preprocessing step may be required, including spatial subsampling, noise removal, or both. Spatial subsampling involves reducing the number of points to facilitate handling the point cloud, by specifying the minimum

distance between two points. Noise removal entails eliminating unnecessary points, such as trees, artifacts, or other irrelevant environmental features.

3.2 Segmentation

Following the preprocessing, the point cloud is segmented to detect the floor and ceiling. For this purpose, we employ the well-known *RANSAC* algorithm used to estimate the best fitting plane. Properly tuning the parameters of the *RANSAC* algorithm, including minimum number of points for a model, iteration count, and distance threshold, is essential for achieving the best results given their impact on accuracy, computation time, and robustness in noisy data.

3.3 Level deviation analysis

Next in line is to calculate level deviation, which denotes the vertical deviation from the actual position of point, line, or plane, concerning the basic position of a reference horizontal plane. Level evaluation is analysed for both single-storey (figure 1.a) and multi-storey (figure 1.b) buildings. Since both the floor and the ceiling are expected to be flat, we use *RANSAC*-based point fitting techniques for creating each plane to extract their parameters. Moreover, we employ equation 1 (where A, B, C and D are the plane parameters and x, y and z are each point coordinates) to calculate the distance (d) from each point (P) to the fitted plane (π) to evaluate the level deviation.

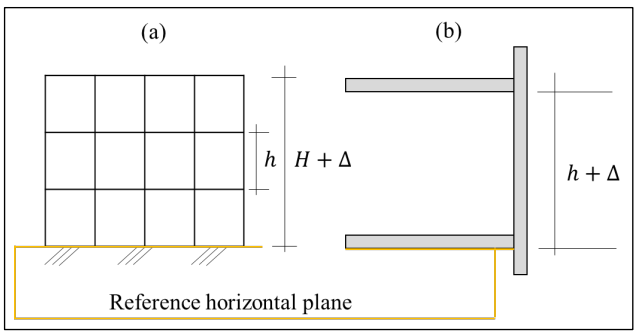

Figure 1. Level deviation analysis. (a) Multi-storey building, (b) Single-storey. H is the total height of the building; h is the height of each floor and Δ is the admitted tolerance.

$$d\,(P,\pi) = \frac{|Ax + By + Cz + D|}{\sqrt{A^2 + B^2 + C^2}} \quad (1)$$

Assuming that the fitted planes represent the real surfaces of the floor and the ceiling, we must only consider the distances that define the usable space between them to verify the height according to the standards. The points within the functional space are positioned above the fitted floor plane and below the fitted ceiling plane (green coloured crosses in figure 2), allowing us to dismiss irrelevant points outside these boundaries. This process requires spatially distributing the level deviation measurements across the entire horizontal surface of the floor plan by projecting the points on the plane and extracting the sign of each calculated distance.

Additionally, the final step in level deviation analysis involves checking the parallelism of both planes using dot product definition and once confirmed, the distance between the planes is calculated to assess any deviation employing equation 2 (where A, B and C are coefficients that define the normal vector and $D1$ and $D2$ represent the offsets of each plane concerning the origin of the coordinates). The distance between planes is considered a deviation if it exceeds the limit bounds imposed by the normative tolerance, which are calculated as follows: the lower bound is [real height - tolerance] while the upper bound is [real height + tolerance]. The error committed by fitting the planes is taking into account if it exceeds the tolerance.

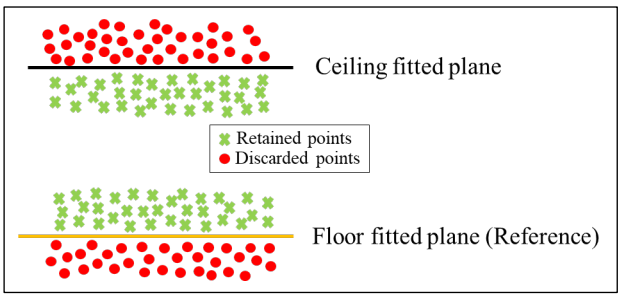

Figure 2. Spatial distribution of points relative to the fitted planes.

$$d\,(\pi_1,\pi_2) = \frac{|D_2 - D_1|}{\sqrt{A^2 + B^2 + C^2}} \quad (2)$$

3.4 Flatness deviation analysis

After that, we implement an algorithm for analysing flatness deviation, which measures how closely a surface approaches to a plane (figure 3). In this case, the plane considered is horizontal, as we are evaluating deviations for both floor and ceiling. Building upon the spatial distribution of points established in the previous analysis, the next step in flatness deviation assessment is to verify whether the distances are within the global tolerance specified on the standards. To accomplish this, the studied surface must be divided into regions of 2×2 square meters, as the requirement applies to every 2-meter length of the surface.

To proceed with this division, the point cloud surface is aligned with the global coordinates by employing the rotation matrix, which is obtained from its covariance matrix, calculated as shown in equation 3 (where X_i and Y_i are the coordinates of the ith point, $\bar{X}$ and $\bar{Y}$ are the mean values for each coordinate and n is the number of points in the point cloud). Afterwards, the limits of each square are calculated, and the points of the surface are iteratively processed accordingly by selecting those that fall within every individual square. Once all of the points are organized, the previously obtained distances between the points and the plane (equation 1) are checked. The verification process involves calculating the mean distance value for the points within each square and ensuring that the result falls within the accepted tolerance.

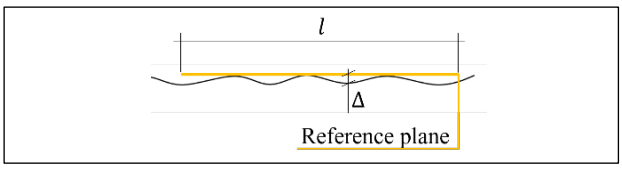

Figure 3. Flatness deviation analysis.

$$cov(X,Y) = \frac{\sum_{i=1}^{n}(X_i - \bar{X})(Y_i - \bar{Y})}{n-1} \quad (3)$$

3.5 Vertical deviation analysis

Moving forward, our attention turns to analysing the vertical deviation in walls and columns. Vertical deviation is the discrepancy between the position of a point, line, or plane and the

basic position of a vertical line or vertical plane reference (figure 4). We proceed to segment the provided elements vertically into sections, specifying the height of each segment. After obtaining the vertical sections of the point cloud for the element, we determine its centroid by calculating the mean of each coordinate of the points in the cloud.

Ultimately, to check if the element is vertically aligned, we have to select a reference, specifically the reference centroid. Initially it seems logical to select the lower centroid. However, after testing with different elements, we have noticed deviations in the extreme centroids that could lead false negatives. Consequently, the second lowest centroid is chosen as reference, achieving more realistic results.

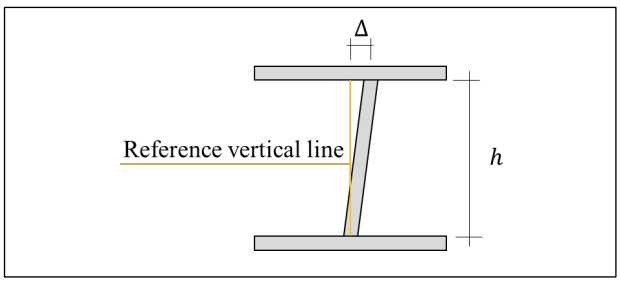

Figure 4. Vertical deviation analysis.

Then, we calculate the transversal distance between the reference centroid and the highest centroid, taking into account that the verification process differs depending on whether the element is a column or a wall. If the element is a column, we measure the distance in both *x* and *y*-coordinates (figure 5.a), while if the element is a wall we only calculate the deviation in the direction of the normal vector (figure 5.b). Initially, we determine the orientation of the wall by fitting a plane. Then, the normal vector is obtained from the fitted plane parameters, and we proceed to calculate the distance in the established direction, obtaining the deviation.

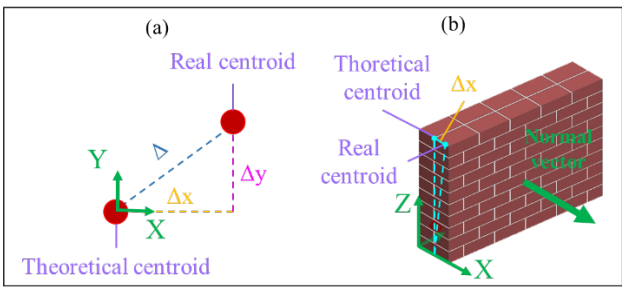

Figure 5. Transversal distance calculation: (a) For columns, (b) For walls.

3.6 Axis deviation of free space between columns analysis

Finally, we analyse the axis deviation, defined as the free distance between adjacent walls or columns, measured at a reference point (figure 6.a), which are the inner faces of the vertical elements. We begin by rotating the point cloud using the procedure established in the flatness deviation analysis. This rotation is necessary to determine the axis along which we calculate the distance between the adjacent elements of the same type. Subsequently, we segment the point cloud vertically and determine the centroids for each segment as in the vertical deviation analysis.

Furthermore, deriving the dimensions of the columns from the point cloud data is crucial for determining the separation between their inner faces by integrating the dimension information with the centroids. The methodology varies depending on whether the column profile is rectangular or circular. For rectangular profiles, we extract the extreme points of the columns to delineate their boundaries and directly acquire dimensional data by calculating the differences between the maximum and the minimum values along each axis. In contrast, for circular profiles, we initially cluster the points using the *DBSCAN* algorithm. Then, it extracts side points, which are the subset of points representing the outer boundary of the cylindrical shape. These side points are used to calculate their bounding to determine the width, depth and height dimensions. These approaches allow us to calculate the Euclidean distance between inner faces, as shown in figure 6.b., where the dimensions/2 represent half the width or the depth of the element, depending on its alignment. Subsequently, if over half of measurements are within the specified threshold, we consider the elements compliant with the standards.

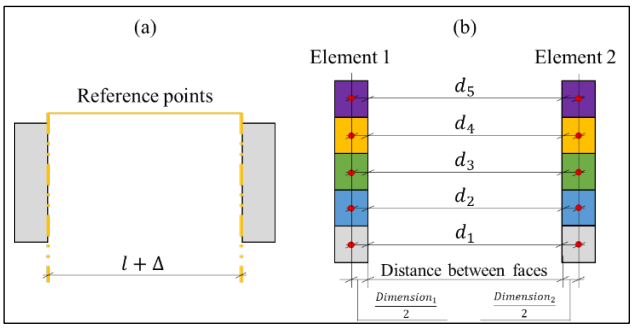

Figure 6. (a) Axis deviation analysis, (b) Measurement between the faces of the columns.

4. Results

4.1 Data acquisition and pre-processing

Finally, we check if the measured distances exceed the tolerances in accordance with the Spanish standard *Real Decreto 470/2021, Annex 14* and the European norm *UNE-EN 13670:2013*, through tests conducted on a real-world case study involving two eight-storey building under construction. The data acquisition of the entire building was conducted using the *BLK2GO* mobile laser scanner, which offers an indoor accuracy of ±10 mm and a range noise of ±3 mm at 25 m, enough for the required accuracy exposed in the standards.

For this study, data from only one of the stories (figure 7.a) was utilized, as it provided sufficient information given the volume of points in the point cloud (312.319.284 points). We began by preprocessing the point cloud, focusing on subsampling to simplify handling, and removing any noisy points (figure 7.b).

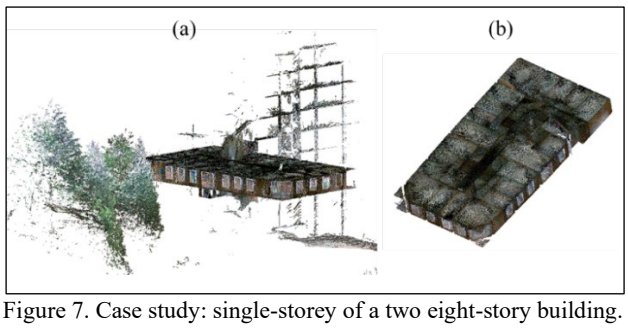

Figure 7. Case study: single-storey of a two eight-story building. (a) Raw point cloud, (b) Pre-processed point cloud

4.2 Segmentation

Subsequently, we proceed with the segmentation of the point cloud into floor, ceiling and walls (Figure 8), employing *RANSAC* algorithm. The parameters were carefully selected to achieve satisfactory results. Specifically, the distance threshold was set to 0.1 m to ensure that points within this range were considered in the fitting process. Additionally, we conducted 10.000 iterations to robustly estimate the best-fitting planes.

Despite the maximum distance might appear to be large, the number of iterations was precisely balanced, allowing the algorithm to effectively converge on high-quality solutions. The number of iterations was carefully adjusted to obtain a compromise between computing time and robustness against the inherent randomness of the algorithm.

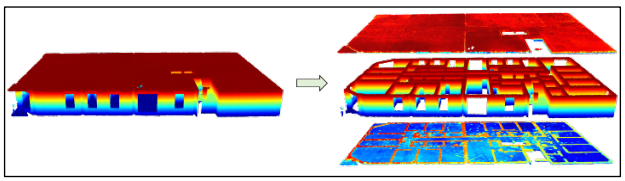

Figure 8. Result of the segmentation process employing *RANSAC* algorithm.

The selection of these parameters involved a series of trial-and-error executions to ensure high reliability and consistency during segmentation. Adopting this detailed approach allowed the segmentation to provide accurate, slice-like delineation of all the major structures, as basis for more discussion under analysis, inspection and validation.

4.3 Level deviation

To introduce the findings from the level deviation, figure 9 shows the spatial distribution of the points, highlighting whether they are positioned above or below their respective fitted plane. Notably, the mean error committed in fitting the floor and ceiling planes is 0.009 m and 0.01 m, in each case, both of which remain below the admitted tolerance of ±0.020 m. This ensures a robust fit without the need to account for plane error during verification.

Furthermore, the mean measured distance between the fitted planes, which amounts to 2.758 m, falls within the bounding box delineated by the theoretical height, 2.741 m, and the admitted tolerance.

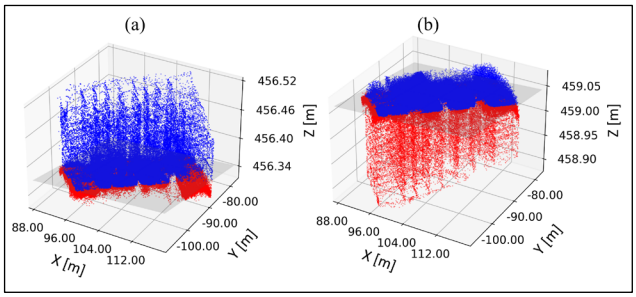

Figure 9. Spatial distribution of points relative to fitted planes. (a) Floor, (b) Ceiling.

4.4 Flatness deviation

In the other hand, respecting to the flatness deviation, after calculating the covariance matrix for each surface, floor and ceiling, we obtained the results illustrated in the graphs of the figure 10.

These results show a positive correlation between x (0) and y (1) coordinates, indicating their tendency to increase together. This correlation is essential for reconstructing an accurate rotation matrix for our point cloud data, as it informs how the points are oriented relative to each other. Additionally, symmetric covariance values further support this, suggesting similar variability in those coordinates.

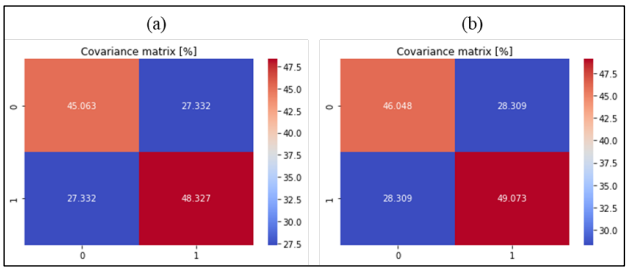

Figure 10. Covariance matrices. (a) Floor, (b) Ceiling.

We continuously extracted the eigenvectors employing eigenvalue decomposition, which allowed us to identify the main directions for variation in the point cloud. The resulting eigenvectors are provided below.

$$\begin{bmatrix} -0.728 & 0.686 \\ 0.686 & 0.728 \end{bmatrix}$$
Floor plane eigenvectors

$$\begin{bmatrix} -0.727 & 0.686 \\ 0.686 & 0.727 \end{bmatrix}$$
Ceiling plane eigenvectors

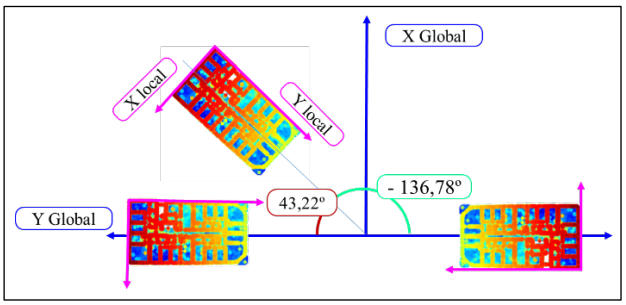

Figure 11. Point cloud alignment procedure.

Then, we selected the eigenvector corresponding to the smallest eigenvalue, representing the direction of least variation. For the floor, the resulting eigenvector was $[-0.723 \quad 0.686]$ and for the ceiling, it was $[-0.727 \quad 0.686]$. These values correspond to a variation angle of 136.78º or -43.22º (figure 11) with respect to the x-axis in both cases. The resulting rotation matrices obtained are as follows.

$$\begin{bmatrix} -0.728 & -0.686 & 0 \\ 0.686 & -0.728 & 0 \\ 0 & 0 & 1 \end{bmatrix}$$
Floor rotation matrix

$$\begin{bmatrix} -0.727 & -0.686 & 0 \\ 0.686 & -0.727 & 0 \\ 0 & 0 & 1 \end{bmatrix}$$
Ceiling rotation matrix

Once the point cloud was aligned with the global coordinates, we divided both surfaces in 2x2 meters squares. We required eight squares along the local x-axis and 14 along the local y-axis, resulting in a total of 120 squares. To enhance visualization, every individual square is represented in a random colour (figure 12.a and figure 12.b). Moreover, each square has been assigned an ID for identification. The initial square, coinciding with the local coordinate axis (0,0), is located in the bottom-right corner and the values increase while advancing along the axes.

Finally, we verified every square by checking if the mean distance between the points within each square and the fitted plane complied with the admitted global tolerance of ±0.015 m, corresponding with *Unmoulded surface*. In figure 12.c and 12.d, compliant squares are coloured in green, while non-compliant ones, (3,7) and (4, 10) on the floor and (4, 0), (4, 13), (5, 5), (5, 8), (6, 5) and (6, 9) on the ceiling, are shown in red. In figure 13, the distance scattering for the flatness assessment is illustrated, revealing a maximum deviation of 0.024 m on the ceiling, representing a 60% increase over the permitted deviation, and a 33% increase on the floor. Additionally, a notable number of measurements show deviations exceeding 50%, underscoring the variability present in the data.

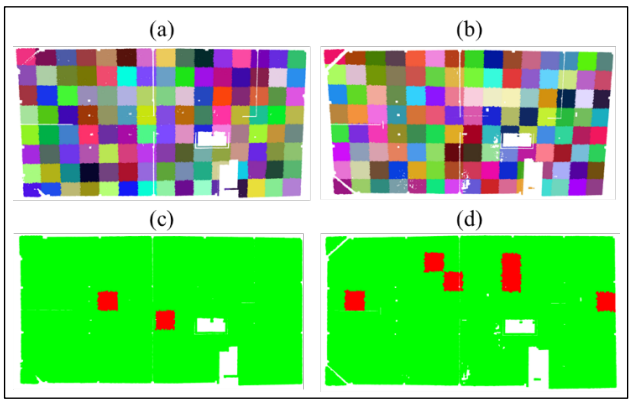

Figure 12. Segmentation into 2x2 square meters: (a) Floor, (b) Ceiling. Verification: (c) Floor, (d) Ceiling.

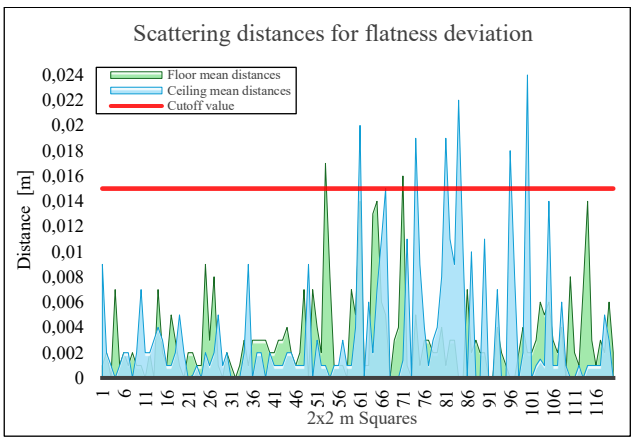

Figure 13. Scattering distance for flatness deviation analysis on floor and ceiling

4.5 Vertical deviation

The next phase in our quality control method is the analysis of the vertical deviation. If the height is less than or equal to 6 m, the allowed deviation is ±24 mm. If the height is in the range of 6 m to 30 m, the deviation increases ±4 times the height in millimetres, ensuring it does not surpass ±50 mm. For heights exceeding 30 m, the permitted deviation is ±5 times the height divided by 3 in millimetres, constrained within ±150 mm. Considering the height of our case study to be 2.741 m, the allowable deviation for the vertical elements is limited to ±24 mm.

In figure 14 we present the results for vertical deviation in two adjacent columns of the presented case study. First, we sectioned the elements into 55 vertical segments of 0.05 m of height, a parameter chosen based on experimentation. Shorter segments resulted in an excessive number of centroids, risking clarity visualization, while larger ones lacked structural detail. After examining both *x* and *y* axes for the columns, we found that in column 1 the deviation on the *x*-axis was 0.074 m and on the *y*-axis was 0.020 m. As a result, column 1 fails to meet the specified criteria in the *x* direction, making it non-compliant, despite satisfying them in the *y* direction. Conversely, in column 2, the *x*-axis deviation was 0.041 m, and the *y*-axis deviation was 0.165 m, resulting in failure to meet the specified criteria in both directions.

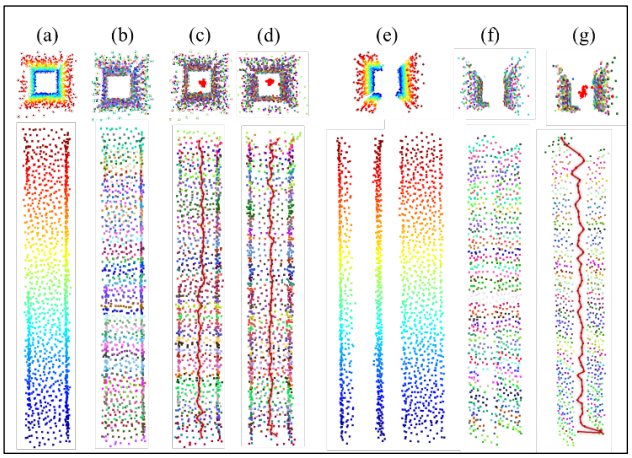

Figure 14. Vertical deviation analysis in columns results. (a) Column 1, (b) Column 1 vertical partitioning, (c) Column 1 centroids alignment along *x*-*z* plane, (d) Column 1 centroids alignment along *y*-*z* plane, (e) Column 2, (f) Column 2 vertical partitioning, (g) Column 2 centroids alignment in perspective

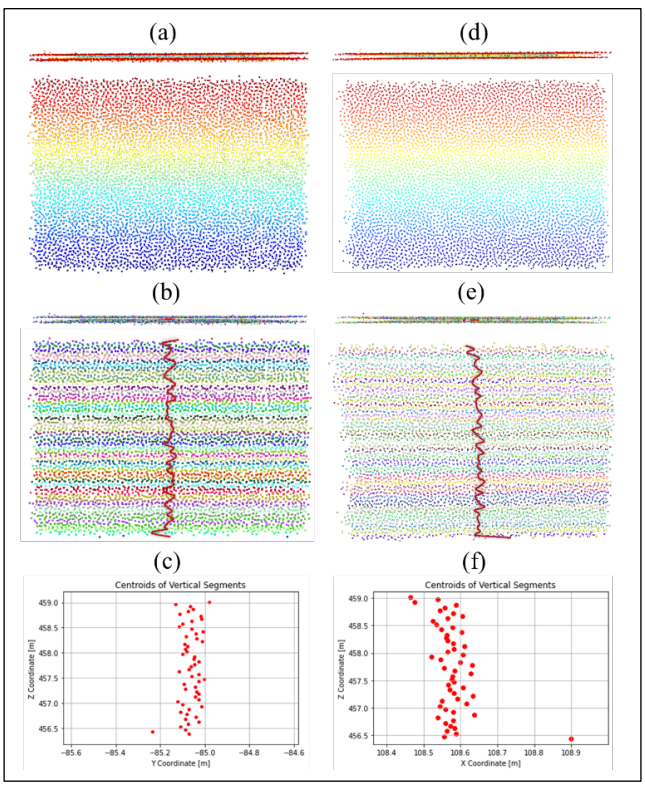

Figure 15. Vertical deviation analysis in walls results. (a) Wall 1 (*x*-axis orientation), (b) Wall 1 centroids alignment along *x*-*z* plane, (c) Wall 1 centroids alignment along *y*-*z* plane, (d) Wall 2 (*y*-axis orientation) (e) Wall 2 centroids alignment along *x*-*z* plane, (f) Wall 2 centroids alignment along *x*-*z* plane.

The analysis then shifted to evaluating the vertical deviation of two walls (figure 15), each divided in 54 vertical sections of 0.05 m of height. After fitting a plane to each one, we determined that wall 1 is orientated along *x*-axis and wall 2 is orientated along *y*-axis, so we have to check verticality in the *y*-axis for wall 1 and in the *x*-axis for wall 2. The analysis showed a 36 mm deviation in wall 1, failing compliance with the standard, while wall 2, with a deviation of 12 mm, is undistorted.

4.6 Axis deviation of free space between columns

The remaining analysis to verify is the free space between columns. According with the Standards, the maximum permissible deviation for this assessment is determined by the larger value between 20 mm and *l*/600 mm (where *l* represents the distance between reference points in millimetres), ensuring it does not exceed 60 mm.

In our case study, the distance between the reference points of column 1 and column 2 is 6.266 m, resulting in an admitted tolerance of ±0.020 m. Using this data, we establish a bounding box of [6.246, 6.286] m. Figure 16 shows the measurements of the free space between the columns, ranging from 6.227 m to 6.411 m, with a maximum deviation of 2%. Those measured values falling within the bounding box (represented in orange) are highlighted in green, while those outsides are marked in red. Notably, consistent with our previous discussion, values closer to the extremes exhibit a higher degree of deviation.

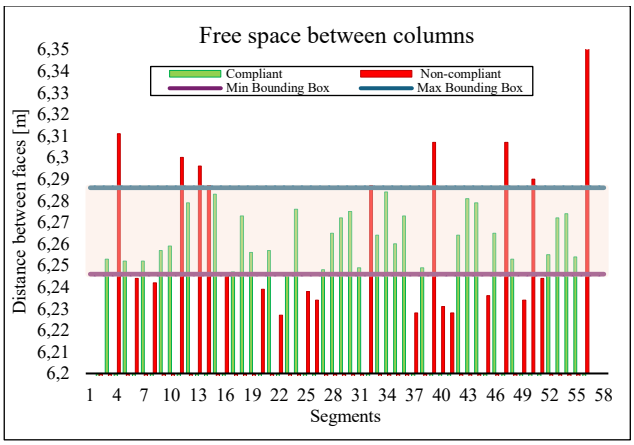

Figure 16. Measured distance between column 1 and column 2 for axis deviation analysis.

5. Conclusions

In this paper, we have described and demonstrated a simple methodology for rapid geometric quality control of buildings under construction from point cloud data obtained with indoor mobile mapping scanners. By adhering to the European norms and Spanish standards, our approach enables the timely detection of deviations, ensuring project integrity. Through the implementation of well-known algorithms, we were able to identify and quantify level, vertical, flatness and axis deviation.

Validation through a real-world case study confirmed the ability of the proposed approach to rapidly identify deviations and assess compliance with *Real Decreto 470/2021* and *UNE-UNE 13670:2013*. Notably, our approach achieved mean error levels within acceptable tolerances for floor and ceiling planes, depicting high accuracy that did not require extra errors consideration during verification. However, it is important to acknowledge the limitations of our method, particularly concerning the accuracy of the *BLK2GO*, rated at ±10 mm, which is not enough when measuring flatness deviation for *Moulded or isolated surfaces*, which have a tolerance of ±9 mm. Consequently, specific deviation detection may necessitate the use of a scanner with higher precision.

The study supports the basis for the development of geometric quality control in construction and provides all the necessary groundwork for improving accuracy, efficiency, and compliance with regulations. Besides the current results, there will always be scope for further future work and research in this area for improving integrity control in construction industry. One potential area for research is the use of new sensors coupled to machine-learning algorithms, offering improved accuracy in identifying defect detection and efficiency in project completion timelines. Moreover, exploring other methodologies to detect deviations, such as transversal section deviation, straightness and curvature deviations, offset deviation, or axis deviation on beams, represents an important area for advancement in the field, as there are not many studies focused on these specific deviations.

Additionally, applying real-time verification systems and continuous inspection throughout the construction activities for complex structural components can significantly improve the geometric quality control process in terms of more accurate and efficient predictions and proactive problem-solving.

Acknowledgements

This work was partially supported by human resources grant RYC2020-029193-I funded by MCIN/AEI/10.13039/501100011033 and FSE ‘El FSE invierte en tu futuro’, by grant ED431F 2022/08 funded by Xunta de Galicia, Spain-GAIN, and by the project CNS2022-135730 funded by MCIN/AEI /10.13039/501100011033 and by the European Union NextGenerationEU/PRTR. The statements made herein are solely the responsibility of the authors.

References

Anil, E. B., Tang, P., Akinci, B., & Huber, D., 2013. Deviation analysis method for the assessment of the quality of the as-is building information models generated from point cloud data. *Automation in Construction*, 35, 507-516. doi.org/10.1016/j.autcon.2013.06.003.

Akinci, B., Boukamp, F., Gordon, C., Huber, D., Lyons, C., Park, K., 2006. A formalism for utilization of sensor systems and integrated project models for active construction quality control. *Automation in Construction*, 15 (2), 124-138. doi.org/10.1016/j.autcon.2005.01.008.

Bueno, M., Bosché, F., 2022. Pre-Processing and Analysis of Building Information Models for Automated Geometric Quality Control. *39th International Symposium for Automation and Robotics in Construction*, Bogotá.

Chen, J., & Cho, Y., 2018. Point-to-point comparison method for automated scan-vs-BIM deviation detection. *International Conference on Computing in Civil and Building Engineering*, Tamper.

Dabrowski, P.S., 2022. Novel PCSE-based approach of inclined structures geometry analysis on the example of the Leaning

Tower of Pisa. *Measurement*, 189, 110462. doi.org/10.1016/j.measurement.2021.110462.

Dąbrowski, P.S., Hubert Zienkiewicz, M., 2022. Impact of cross-section centers estimation on the accuracy of the point cloud spatial expansion using robust M-estimation and Monte Carlo simulation. *Measurement*, 189, 110436. doi.org/10.1016/j.measurement.2021.110436.

Dabrowski, P.S., Zienkiewicz, M.H., Truong-Hong, L., Lindenbergh, R., 2023. Assessing historical church tower asymmetry using point cloud spatial expansion. *Journal of Building Engineering*, 75, 107040. doi.org/10.1016/j.jobe.2023.107040.

Delval, T., Rezoug, M., Tual, M., Fathy, Y., Mege, R., 2023. Towards a digital twin system design based on a user- cantered approach to improve quality control on construction sites. *ICCCBE*.

Fu, L., Xing, Z., Cheng, G., Li, D., Cui, N., Frank Chen, Y., 2022. Terrestrial laser scanning assisted dimensional quality assessment for space frame components. *Measurement,* 204, 112067. doi.org/10.1016/j.measurement.2022.112067.

Girardeau-Montaut, D., Roux, M., Marc, R., Thibault, G., 2005. Change detection on point cloud data acquired with a ground laser scanner. *International Archives of Photogrammetry, Remote Sensing and Spatial Information,* Sciences 36, pp. 30-35.

Jingmond, M., Ågren, R., 2015. Unravelling causes of defects in construction. *Construction Innovation*, 15, 198-218. doi.org/10.1108/CI-04-2014-0025.

Kim, M., Chang, C., 2014. Localization and Quantification of Concrete Spalling Defects Using Terrestrial Laser Scanning. *Journal of Computing in Civil Engineering*, 29, 04014086. doi.org/10.1061/(ASCE)CP.1943-5487.0000415.

Li, D., Liu, J., Hu, S., Cheng, G., Li, Y., Cao, Y., et al., 2022. A deep learning-based indoor acceptance system for assessment on flatness and verticality quality of concrete surfaces. *Journal of Building Engineering,* 51, 104284. doi.org/10.1016/j.jobe.2022.104284.

Matthews, J., Ika, L., Teo, P., Fang, W., Morrison, J., 2021. From Quality-I to Quality-II: cultivating an error culture to support lean thinking and rework mitigation in infrastructure projects. *Production Planning & Control* 34 1-18. doi.org/10.1016/j.eng.2022.05.010.

Ministerio de Transportes, Movilidad y Agenda Urbana, 2021: Real Decreto 470/2021, June 29. *Boletín Oficial del Estado* (*BOE*). Available At: https://www.boe.es/eli/es/rd/2021/06/29/470.

Mirzaei, K., Arashpour, M., Asadi, E., Masoumi, H., Mahdiyar, A., & Gonzalez, V., 2023a. End-to-end point cloud-based segmentation of building members for automating dimensional quality control. *Advanced Engineering Informatics*, 55, 101878. doi.org/10.1016/j.aei.2023.101878.

Mirzaei, K., Arashpour, M., Asadi, E., Feng, H., Mohandes, S. R., & Bazli, M., 2023b: Automatic compliance inspection and monitoring of building structural members using multi-temporal point clouds. *Journal of Building Engineering*, 72, 106570. doi.org/10.1016/j.jobe.2023.106570.

Moyano, J., Gil-Arizón, I., Nieto-Julián, J.E., Marín-García, D., 2022. Analysis and management of structural deformations through parametric models and HBIM workflow in architectural heritage. *Journal of Building Engineering*, 45, 103274. doi.org/10.1016/j.jobe.2021.103274

Mohammadi, M.E., 2019. Point Cloud Analysis for Surface Defects in Civil Structures. *ETD collection for University of Nebraska-Lincoln*, AAI22616444. Available at: https://digitalcommons.unl.edu/dissertations/AAI22616444.

Park, S., Ju, S., Yoon, S., Nguyen, M. H., & Heo, J., 2021. An efficient data structure approach for BIM-to-point-cloud change detection using modifiable nested octree. *Automation in Construction*, 132, 103922. doi.org/10.1016/j.autcon.2021.103922.

P. E. Love, J. Matthews, M. C. Sing, S. R. Porter & W. Fang, 2022: State of Science: Why Does Rework Occur in Construction? What Are Its Consequences? And What Can be Done to Mitigate Its Occurrence? *Engineering, 1*8, 246-258. doi.org/10.1016/j.eng.2022.05.010.

Spencer, B.F., Hoskere, V., Narazaki, Y., 2019. Advances in Computer Vision-Based Civil Infrastructure Inspection and Monitoring. *Engineering*, 5 (2), 199-222. doi.org/10.1016/j.eng.2018.11.030.

Suchocki, C., Damięcka-Suchocka, M., Jagoda, M., 2008. Determination of the building wall deviations from the vertical plane. In Proceedings of the *7th International Conference on Environmental Engineering*, *ICEE*, Vilnius.

AEN/CTN 83 Technical Committee, 2013. UNE-EN 13670: Execution of concrete structures. *Aenor*. Avilable at: www.une.org.